

# Determination of TG-43 Dosimetric Parameters for Photon Emitting Brachytherapy Sources

Mozaffari A.<sup>1</sup>, Ghorbani M.<sup>1\*</sup>

## ABSTRACT

**Objective:** Brachytherapy sources are widely used for the treatment of cancer. The report of Task Group No. 43 (TG-43) of American Association of Physicists in Medicine is known as the most common method for the determination of dosimetric parameters for brachytherapy sources. The aim of this study is to obtain TG-43 dosimetric parameters for  $^{60}\text{Co}$ ,  $^{137}\text{Cs}$ ,  $^{192}\text{Ir}$  and  $^{103}\text{Pd}$  brachytherapy sources by Monte Carlo simulation.

**Methods:** In this study,  $^{60}\text{Co}$  (model Co0.A86),  $^{137}\text{Cs}$  (model 6520-67),  $^{192}\text{Ir}$  (model BEBIG) and  $^{103}\text{Pd}$  (model OptiSeed) brachytherapy sources were simulated using MCNPX Monte Carlo code. To simulate the sources, the exact geometric characterization of each source was defined in Monte Carlo input programs. Dosimetric parameters including air kerma strength, dose rate constant, radial dose function and anisotropy function were calculated for each source. Each input program was run with sufficient number of particle histories. The maximum type A statistical uncertainty in the simulation of the  $^{60}\text{Co}$ ,  $^{137}\text{Cs}$ ,  $^{192}\text{Ir}$  and  $^{103}\text{Pd}$  sources, were equal to 4%, 4%, 3.19% and 6.50%, respectively.

**Results:** The results for dosimetry parameters of dose rate constant, radial dose function and anisotropy function for the  $^{60}\text{Co}$ ,  $^{137}\text{Cs}$ ,  $^{192}\text{Ir}$  and  $^{103}\text{Pd}$  sources in this study demonstrated good agreement with other studies.

**Conclusion:** Based on the good agreement between the results of this study and other studies, the TG-43 results for Co0.A86  $^{60}\text{Co}$ , 67-65200  $^{137}\text{Cs}$ , BEBIG  $^{192}\text{Ir}$  and OptiSeed  $^{103}\text{Pd}$  sources are validated and can be used as input data in treatment planning systems (TPSs) and to validate the TPS calculations.

**Citation:** Mozaffari A, Ghorbani M. Determination of TG-43 Dosimetric Parameters for Photon Emitting Brachytherapy Sources. *J Biomed Phys Eng*. 2019;9(4):425-436. <https://doi.org/10.31661/jbpe.v0i0.570>.

## Keywords

Brachytherapy • TG-43 dosimetric Parameters • Monte Carlo Method •  $^{60}\text{Co}$  •  $^{137}\text{Cs}$  •  $^{192}\text{Ir}$  •  $^{103}\text{Pd}$

## Introduction

There are different treatment methods such as surgery, chemotherapy and radiation therapy for the treatment of cancer. Radiotherapy consists of two main methods including external beam radiation therapy and internal radiation therapy (brachytherapy). Brachytherapy is a method of cancer therapy in which radioactive sources are placed adjacent to the malignant tumors to irradiate them. The tumor can be locally irradiated with a high dose level by this method. In the past,  $^{226}\text{Ra}$  has mainly been used for this purpose. This treatment plays an important role in cancer treatment in different body organs including brain, head

<sup>1</sup>Medical Physics Department, Faculty of Medicine, Mashhad University of Medical Sciences, Mashhad, Iran

\*Corresponding author: M. Ghorbani, Medical Physics Department, Faculty of Medicine, Mashhad University of Medical Sciences, Paradise Daneshgah, Azadi Square., Mashhad, Iran  
E-mail: mhdghorbani@gmail.com

Received: 6 May 2016  
Accepted: 13 June 2016

and neck, prostate, cervix, etc. [1].

Brachytherapy involves two main different treatments: intracavitary and interstitial. In intracavitary, brachytherapy sources are inserted inside the body adjacent to the tumor via body's natural cavities, and irradiate the tumor. In interstitial brachytherapy, radioactive seeds are implanted directly inside the tumor volume. High levels of radiation dose can be delivered with this treatment method and the existing rapid dose fall-off reduces the dose to the healthy tissues around the tumor [2-4]. Brachytherapy sources are widely used for the treatment of malignancies nowadays. Therefore, providing an accurate method to obtain dose distribution around brachytherapy source is of clinical importance.

The report by Task Group No. 43 (TG-43) of American Association of Physicists in Medicine has been known as the most common formalism for obtaining dose distribution around brachytherapy sources and the presented formalism is used in many treatment planning systems (TPSs). According to the report, dose distribution around brachytherapy sources is calculated using a variety of factors which are obtained through measurement or Monte Carlo simulation methods in a uniform phantom [4, 5]. Based on the recommendations by this report, dosimetry parameters of brachytherapy sources should be determined by two independent researchers for the purpose of clinical use. Various studies have been conducted for the calculation of dosimetry parameters of different models of brachytherapy sources [6-8]. The aim of this study is to determine dosimetry parameters of  $^{60}\text{Co}$  (model Co0.A86),  $^{137}\text{Cs}$  (model 6520-67),  $^{192}\text{Ir}$  (model BEBIG) and  $^{103}\text{Pd}$  (model OptiSeed) sources.

## Materials and Methods

### Source Geometries

In this study, four sources including  $^{60}\text{Co}$  (model Co0.A86),  $^{137}\text{Cs}$  (model 6520-67),  $^{192}\text{Ir}$  (model BEBIG) and  $^{103}\text{Pd}$  (model OptiSeed)

were chosen. Figure 1 (part (a)) shows the design of BEBIG  $^{60}\text{Co}$  source. This source has been made from a cylindrically shaped central core containing  $^{60}\text{Co}$  with length of 5.3 mm and diameter of 5.0 mm. The core is placed inside a cylindrical capsule with 7.0 mm inner diameter and 1 mm outer diameter. The length of the cable is equal to 5 mm in this source model [9].

Figure 1 (part (b)) shows the schematic diagram of 6520-67  $^{137}\text{Cs}$  source. The active part of the source is 14.8 mm in length and 1.52 mm in diameter. The radioactive  $^{137}\text{Cs}$  is uniformly distributed in the core of the source in the form of cesium oxide ceramic. The density of the active material is  $1.47 \text{ g/cm}^3$ . The core is located inside a capsule made of stainless steel. The density of the stainless steel is equal to  $7.9 \text{ g/cm}^3$  [10].

A schematic view of the BEBIG  $^{192}\text{Ir}$  source is shown in Figure 1 (part (c)).  $^{192}\text{Ir}$  source is composed of a cylindrically active core with active length of 3.5 mm and an diameter of 0.6 mm. The active core is covered by a 316L stainless steel capsule [6].

Regarding OptiSeed  $^{103}\text{Pd}$  source, the active part is composed of two active pellets, each in the form of a cylinder with 0.7 mm diameter and 0.4 mm length. The central part of the source is made of gold marker with 2 mm in length and 0.4 mm in diameter [11]. Figure 1 (part (d)) shows a schematic diagram of the OptiSeed  $^{103}\text{Pd}$  source.

The energy spectrum used in this study for the  $^{60}\text{Co}$  source is 1.33 and 1.17 MeV, each energy with 0.5 probability. The energy spectra of  $^{137}\text{Cs}$ ,  $^{192}\text{Ir}$  and  $^{103}\text{Pd}$  sources are presented in Table 1.

### TG-43 Formalism

According to TG-43 report for brachytherapy sources, dose distribution can be described based on a polar coordinate system whose origin is located at the center of source. Based on this formalism,  $P(r, \theta)$  is the point of interest and for this point  $r$  is the distance from the

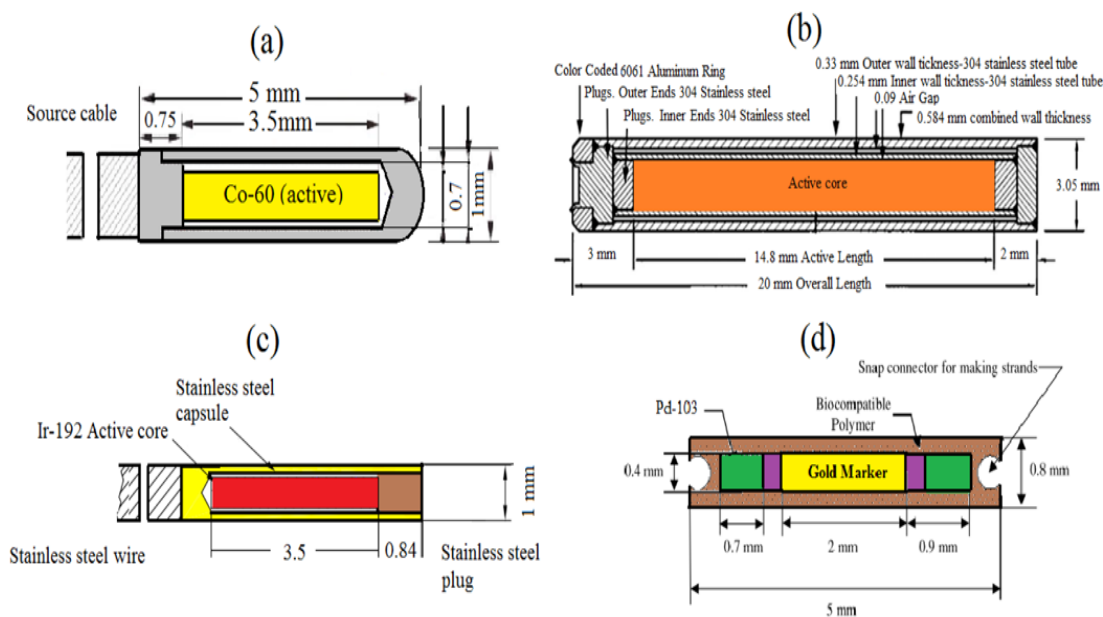


**Figure 1:** A schematic diagram illustrating the geometry of (a): <sup>60</sup>Co source (model Co0.A86); (b): <sup>137</sup>Cs source (model 67-65200); (c): <sup>192</sup>Ir source (model BEBIG); and (d): <sup>103</sup>Pd source (model OptiSeed). This figure is not plotted in a real scale, but the dimensions are in millimeter.

point from the origin and  $\theta$  is the polar angle.  $P(r_0, \theta_0)$  is the reference point, with  $r_0 = 1$  cm and  $\theta_0 = \pi/2$  as the reference coordination.

Dose rate at the point  $P(r, \theta)$  in the water is obtained from the following equation:

$$\dot{D}(r, \theta) = S_K \Lambda \frac{G(r, \theta)}{G(r_0, \theta_0)} g(r) F(r, \theta) \quad (1)$$

where:

$r$ : is the distance of point P from the origin in terms of cm;

$\theta$ : is the polar angle between the source longitudinal axis and the line which connects the point of interest to the source's center;

$S_K$ : is air kerma strength ( $\text{cGycm}^2\text{h}^{-1}(\text{U})$ );

$\Lambda$ : is dose rate constant in water ( $\text{cGyh}^{-1}\text{U}^{-1}$ );

$G_L(r, \theta)$ : is geometry function;

$g_L(r)$ : is radial dose function; and

$F(r, \theta)$ : is anisotropy function;

Dose rate constant is calculated from the following equation:

$$\Lambda = \frac{\dot{D}(r_0, \theta_0)}{S_K} \quad (2)$$

Radial dose function is obtained from this formula:

$$g_L(r) = \frac{\dot{D}(r, \theta_0) G(r_0, \theta_0)}{\dot{D}(r_0, \theta_0) G(r, \theta_0)} \quad (3)$$

According to the TG- 43 formalism, anisotropy function for a brachytherapy source is obtained from the equation (4) as follows:

$$F(r, \theta) = \frac{\dot{D}(r, \theta) G_L(r, \theta_0)}{\dot{D}(r, \theta_0) G_L(r, \theta)} \quad (4)$$

### Monte Carlo Simulations

#### <sup>60</sup>Co Source Simulations

To calculate the air kerma strength for <sup>60</sup>Co source, torus cells with 1 mm thickness were considered at a distance of 30 cm from the

**Table 1:** The energy spectra of  $^{137}\text{Cs}$ ,  $^{192}\text{Ir}$  and  $^{103}\text{Pd}$  radionuclides

$^{137}\text{Cs}$		$^{192}\text{Ir}$		$^{103}\text{Pd}$	
Energy (keV)	Intensity (%)	Energy (keV)	Intensity (%)	Energy (keV)	Intensity (%)
4.47	0.914	9.44	3.9216	2.7	8.7321
31.817	1.995	65.122	2.626	20.074	22.47
32.194	3.641	66.831	4.441	20.216	42.512
36.304	0.3489	75.368	0.53111	22.699	3.541
36.378	0.67218	75.749	1.02122	22.724	6.8519
37.255	0.2136	77.831	0.3648	23.172	1.645
283.51	0.00059	136.393	0.19925	39.7488	0.0683
661.6573	85.102	176.984	0.00431	53.291	$3.0 \times 10^{-5}$
		280.2724	0.0084	62.413	0.001044
		295.9565	28.72	241.885	$5.0 \times 10^{-7}$
		308.45507	29.707	294.9815	0.002807
		316.50618	82.86	317.725	$1.5 \times 10^{-5}$
		416.46887	0.67021	357.458	0.02217
		468.06885	47.843	443.795	$1.5 \times 10^{-5}$
		485.456	0.00474	497.0801	0.003961
		588.58107	4.5221		
		593.6319	0.04201		
		599.4115	0.003917		
		604.41105	8.21619		
		612.46215	5.347		
		765.83	0.00136		
		884.53657	0.2927		
		1061.494	0.05316		
		1089.9626	0.0011616		
		1378.5024	0.0014019		

source. Inside the torus was defined air and the outside was defined as vacuum. An energy cutoff of 10 keV was used for both photons and electrons. The number of photon histories simulated was  $5 \times 10^6$  to obtain air kerma rate and the F6 tally (MeV/g) was used to score air kerma. The statistical uncertainty for this simulation program was 0.63%. To calculate the air kerma strength, the F6 output was multiplied by a number of factors which are given in equation (5).

$$S_K \text{ per activity (cGycm}^2\text{h}^{-1}\text{Bq}^{-1}) = \text{MC output (MeV/g per photon)} \times d^2 \text{ (cm}^2) \times 10^6 \text{ (eV/MeV)} \times 1.602 \times 10^{-19} \text{ (J/eV)} \times 10^3 \text{ (g/kg)}$$

$$\times 100 \text{ (cGy/Gy)} \times 1 \text{ Bq} \times 1 \text{ (dis/s per Bq)} \times \text{photon yield (photons/dis)} \times 3600 \text{ (s/h)} \quad (5)$$

According to TG-43 formalism, to calculate the dose rate constant of the  $^{60}\text{Co}$  source, a torus cell was defined at a distance of 1 cm from the source with a thickness of 0.1 mm. The medium inside the torus was defined as water. To create the conditions of full scattering, a water phantom with a radius of 100 cm was defined. \*F8 tally was used in this program to calculate the energy deposition, and the energy deposition value was divided by the mass of the cell. The number of photon histories simulated was  $6 \times 10^6$ . The Monte Carlo statistical uncertain-

ty equals 2.2% in this simulation. According to equation (2), to calculate dose rate constant parameter, the obtained dose value was divided to air kerma strength.

According to the instructions by TG-43, the values of radial dose function for a source must be calculated on the transverse plane ( $\theta_0 = \pi/2$ ) in different radial distances from the source. For this purpose, tori with 0.1 mm thickness at distances of  $r \leq 1$  cm from the source, tori with 0.5 mm thickness at distances of  $1 < r \leq 5$  cm, tori with 1 mm thickness at distances of  $5 < r \leq 10$  cm and tori with thickness of 2 mm at distances of  $10 < r \leq 20$  cm were defined. The thickness of these tori was defined according to the report by AAPM and ESTRO [12]. Water was defined inside the tori cells and to create the conditions of full scattering, a water sphere with 100 cm radius was defined around the source. Lin source approximation was used in the calculation of geometry function ( $G_L(r, \theta)$ ). To score energy deposition inside tori cells \*F8 tally was used. The number of photon histories simulated was  $60 \times 10^6$  photons and the maximum type A uncertainty in the Monte Carlo calculation equals 2.2%. According to TG-43 formalism, the radial dose function of the brachytherapy source was obtained from equation (3).

To calculate the anisotropy function for the  $^{60}\text{Co}$  source, a water phantom with 100 cm radius was defined. Based on TG-43 report, anisotropy function values should be calculated at different distances and polar angles around a source. For this purpose, for  $^{60}\text{Co}$  source, tori with 0.1 mm thickness at distances of  $r \leq 1$  cm from the source, tori with 0.5 mm thickness at distances of  $1 < r \leq 5$  cm, tori with 1 mm thickness at distances of  $5 < r \leq 10$  cm and tori with thickness of 2 mm at distances of  $10 < r \leq 20$  cm were defined. The thicknesses of these torus cells were based on the recommendations by the report of AAPM and ESTRO. To calculate this parameter, angles were selected in the range of 0 to 180 degrees. For zero-degree angle, because it was not possible to define a

torus with a radius of zero, spheres were used instead of torus. At these points (zero angle), due to lower volume of tally cells in the form of spheres, the statistical uncertainty of Monte Carlo calculations was higher. Since there was overlapping between the sphere and tori, some data points were missing. To avoid this phenomenon, a separate program was written and run for the zero-degree angle. The energy flux was scored in the spherical and torus tally cells using \*F4 tally. In the calculation dose, mass energy absorption coefficient was utilized to convert the energy flux to absorbed dose. The number of photon histories simulated in each program was  $3 \times 10^6$  and the maximum statistical uncertainties for the sphere and tori cells programs were equal to 4% and 2.3%, respectively.

#### $^{137}\text{Cs}$ Source Simulations

To calculate TG-43 parameters of  $^{137}\text{Cs}$  source, the calculation conditions such as voxel size, phantom size, etc. were similar to the calculation for  $^{60}\text{Co}$  source. However, the statistical uncertainty in calculation of air kerma strength parameter was equal to 1.2%. Maximum Monte Carlo statistical type A uncertainty for calculation of radial dose function parameter was equal to 3.4% and for calculation of anisotropy function for all angles except 0 and 180 degrees was equal to 2.3%. The uncertainty for 0 and 180 degrees was equal to 4% and 7.3%, respectively. The Co0.A86  $^{60}\text{Co}$  source geometry and energy spectrum were defined in the simulations.

#### $^{192}\text{Ir}$ Source Simulations

To calculate TG-43 dosimetry parameters for  $^{192}\text{Ir}$  source, the methods provided for the  $^{60}\text{Co}$  source was used but with difference that energy cutoff of 5 keV was used for both photons and electrons.

#### $^{103}\text{Pd}$ Source Simulations

To calculate the air kerma strength for the  $^{103}\text{Pd}$  source, a torus with thickness of 0.15 mm at distance of 30 cm from the source was considered. Energy cutoff of 1 keV was used for both photons and electrons. Type A statis-

tical uncertainty for this simulation program was 2.09%.

To calculate the dose rate constant of OptiSeed  $^{103}\text{Pd}$  source, the number of photon histories simulated was  $3.0 \times 10^8$  in calculation of absorbed dose. Energy cutoff of 1 keV was used for both photons and electrons. The Monte Carlo statistical uncertainty equals 1.6% in this program.

To calculate the radial dose function of the  $^{103}\text{Pd}$  source, tori with 0.1 mm thickness at 0.1-1 cm distances from the source, tori with 0.5 mm thickness at 1.5, 2, 3, 4 and 5 cm distances from the source were defined. Energy cutoff of 1 keV was used for both photons and electrons. The number of photon histories simulated was  $3.0 \times 10^8$  in calculation of dose. Maximum Monte Carlo statistical uncertainty equals 2.3%.

To calculate the anisotropy function for the  $^{103}\text{Pd}$  source tori with 0.1 mm thickness for  $r \leq 1$  cm distances from the source, tori with 0.5 mm for  $1 < r \leq 5$  cm distances, and tori with 1 mm thickness for  $5 < r \leq 10$  cm distances from the source were considered. Due to the symmetrical shape of the source, only angles in the range of 0 to 90 degrees were selected. Energy cutoff of 1 keV was used for both photons and electrons. The number of photon histories simulated was  $3.0 \times 10^8$ . Maximum Monte Carlo statistical uncertainty for anisotropy function calculation for all angles except 0 degree was equal to 2.1%. This uncertainty for 0 degree was equal to 6.5%.

## Results

The results of air kerma strength for the Co0.A86  $^{60}\text{Co}$ , 67-65200  $^{137}\text{Cs}$ , BEBIG  $^{192}\text{Ir}$  and OptiSeed  $^{103}\text{Pd}$  sources in the study are listed in Table 2. The value of this parameter from another study for Co0.A86  $^{60}\text{Co}$  source is also included in Table 2. The results of dose rate constant for the four sources in this study and from other studies, as well as the percentage differences between these two data sets are provided in Table 3.

**Table 2:** Air-kerma strength per activity ( $\text{cGy}\cdot\text{cm}^2\cdot\text{h}^{-1}\cdot\text{Bq}^{-1}$ ) for the Co0.A86  $^{60}\text{Co}$ , 67-65200  $^{137}\text{Cs}$ , BEBIG  $^{192}\text{Ir}$  and OptiSeed  $^{103}\text{Pd}$  sources.

	Present study	Other studies	Difference (%)
$^{60}\text{Co}$	$3.03 \times 10^{-7}$	$3.046 \times 10^{-7}$ [9]	0.53
$^{137}\text{Cs}$	$7.61 \times 10^{-8}$	-	-
$^{192}\text{Ir}$	$9.48 \times 10^{-8}$	-	-
$^{103}\text{Pd}$	$3.65 \times 10^{-8}$	-	-

**Table 3:** Dose rate constant values ( $\text{cGy}\cdot\text{h}^{-1}\cdot\text{U}^{-1}$ ) for the Co0.A86  $^{60}\text{Co}$ , 67-65200  $^{137}\text{Cs}$ , BEBIG  $^{192}\text{Ir}$  and OptiSeed  $^{103}\text{Pd}$  sources.

	Present Study	Other studies (Reference)	Difference (%)
$^{60}\text{Co}$	1.200	1.087 [9]	3.04
$^{137}\text{Cs}$	0.980	0.948 [10]	3.39
$^{192}\text{Ir}$	1.113	1.119 [6]	-0.53
$^{103}\text{Pd}$	0.707	0.712 [11]	-0.68

In Table 4 the values obtained for radial dose function in this study and other studies and the percentage differences between the two datasets are presented. The radial dose function values for the  $^{60}\text{Co}$  source in this study were compared to the study by Granero, et al. study, and the maximum percentage difference is 6.45%, which is related to the distance of 0.25 cm. The mean absolute difference between these two studies is 3.06%. The radial dose function values for the  $^{137}\text{Cs}$  source in this study were compared to the reported values by Meigooni, et al. The maximum percentage difference between the two studies is 5.74%, which is related to the distance of 7 cm. The mean absolute difference between these two studies is 2.67%. The radial dose function values for the  $^{192}\text{Ir}$  source in this study were compared to those reported by Granero, et al. The maxi-

**Table 4:** Radial dose function values for the Co0.A86  $^{60}\text{Co}$ , 67-65200  $^{137}\text{Cs}$ , BEBIG  $^{192}\text{Ir}$  and Opti-Seed  $^{103}\text{Pd}$  sources

$^{60}\text{Co}$				$^{137}\text{Cs}$			
Distance (cm)	Present Study	Granero, et al. [9]	Difference (%)	Distance (cm)	Present Study	Meigooni, et al. [10]	Difference (%)
0.25	1.072	1.007	6.45	0.25	0.994	1.007	-1.29
0.5	0.998	1.036	-3.70	0.5	1.025	1.003	2.16
0.75	1.006	1.015	-0.86	0.75	0.955	1.002	-4.69
1.0	1.000	1	0.00	1.0	1.000	1.000	0.00
1.5	0.959	0.992	-3.34	1.5	0.963	0.996	-3.32
2.0	0.973	0.984	-1.13	2.0	0.943	0.991	-4.80
3.0	0.916	0.968	-5.35	3.0	0.962	0.981	-1.97
4.0	0.934	0.952	-1.87	4.0	0.936	0.970	-3.52
5.0	0.901	0.936	-3.73	5.0	0.917	0.957	-4.19
6.0	0.894	0.919	-2.74	6.0	0.926	0.943	-1.77
7.0	0.885	0.902	-1.86	7.0	0.875	0.928	-5.74
8.0	0.845	0.884	-4.43	8.0	0.890	0.912	-2.40
10.0	0.819	0.849	-3.49	10.0	0.835	0.876	-4.70
12.0	0.790	0.813	-2.81	12.0	0.808	0.836	0.77
15.0	0.732	0.756	-3.19	15.0	0.742	0.772	0.66
20.0	0.638	0.665	-4.02	20.0	0.651	0.657	-0.87
$^{192}\text{Ir}$				$^{103}\text{Pd}$			
Distance (cm)	Present Study	Granero, et al. [6]	Difference (%)	Distance (cm)	Present Study	Bernard and Vynckier [11]	Difference (%)
0.25	1.003	0.990	1.24	0.1	0.698	0.671	4.08
0.5	0.970	0.996	-2.64	0.15	0.931	0.610	-3.14
0.75	0.963	0.998	-3.59	0.2	1.074	1.117	-3.86
1.0	1.000	1.000	0.00	0.25	1.132	1.196	-5.39
1.5	0.979	1.003	-2.34	0.3	1.209	1.204	0.45
2.0	1.015	1.004	1.13	0.4	1.203	1.246	-3.43
3.0	1.010	1.005	0.46	0.5	1.189	1.239	-4.02
4.0	1.002	1.004	-0.18	0.6	1.136	1.194	-4.89
5.0	1.014	0.999	1.51	0.7	1.109	1.153	-3.78
6.0	0.980	0.992	-1.11	0.8	1.065	1.117	-4.62
7.0	0.959	0.981	-2.24	0.9	1.033	1.055	-2.05
8.0	1.001	0.968	3.36	1	1.000	1.000	0.00
10.0	0.940	0.935	0.52	1.5	0.795	0.795	0.01
12.0	0.910	0.894	1.74	2	0.609	0.637	-4.32
15.0	0.839	0.821	2.15	3	0.351	0.360	-2.44
20.0	0.691	0.687	0.61	4	0.198	0.193	2.47
				5	0.108	0.120	-10.34

imum percentage difference is 3.59%, and this value is related to the distance of 0.75 cm. The mean absolute difference between these two studies is 1.55%. The radial dose function values for the  $^{103}\text{Pd}$  source obtained in this study were compared to the study by Bernard and Vynckier and the maximum percentage difference is -10.39%, at distance of 0.5 cm. The mean absolute difference between these two studies is 3.49%.

Anisotropy function values for the  $^{60}\text{Co}$ ,  $^{137}\text{Cs}$  and  $^{192}\text{Ir}$  sources were calculated for distances in the range of 0.25 cm to 20 cm from the source in different angles (ranging from 0 to 180 degrees). For the  $^{103}\text{Pd}$  source, anisotropy function values were calculated for distances in the range of 0.5 cm to 7 cm from the source in different angles (ranging from 0 to 90 degrees). Figures 2, 3, 4 and 5 show anisotropy function values at different distances for the Co0.A86  $^{60}\text{Co}$ , 67-65200  $^{137}\text{Cs}$ , BEBIG  $^{192}\text{Ir}$  and OptiSeed  $^{103}\text{Pd}$  sources.

In Figure 2, anisotropy function values at different distances for the  $^{60}\text{Co}$  source in this study and Granero, et al. are presented in parts (a) and (b), respectively. The percentage difference between the anisotropy function values of the two studies are shown in Figure 2 (part (c)). The maximum percentage difference between these two studies is 8.38% and the mean absolute percentage difference is 0.80%.

In Figure 3, anisotropy function values at different distances for the  $^{137}\text{Cs}$  source in this study and by Meigooni, et al. are presented in parts (a) and (b), respectively. The percentage differences between the anisotropy function values of the two studies are shown in Figure 3 (parts (c)). The maximum percentage difference is 12.02% and the mean absolute percentage difference between these two studies is 0.85%.

In Figure 4 anisotropy function values at different distances for the  $^{192}\text{Ir}$  source in this study and by Granero, et al. are presented in parts (a) and (b), respectively. The percentage

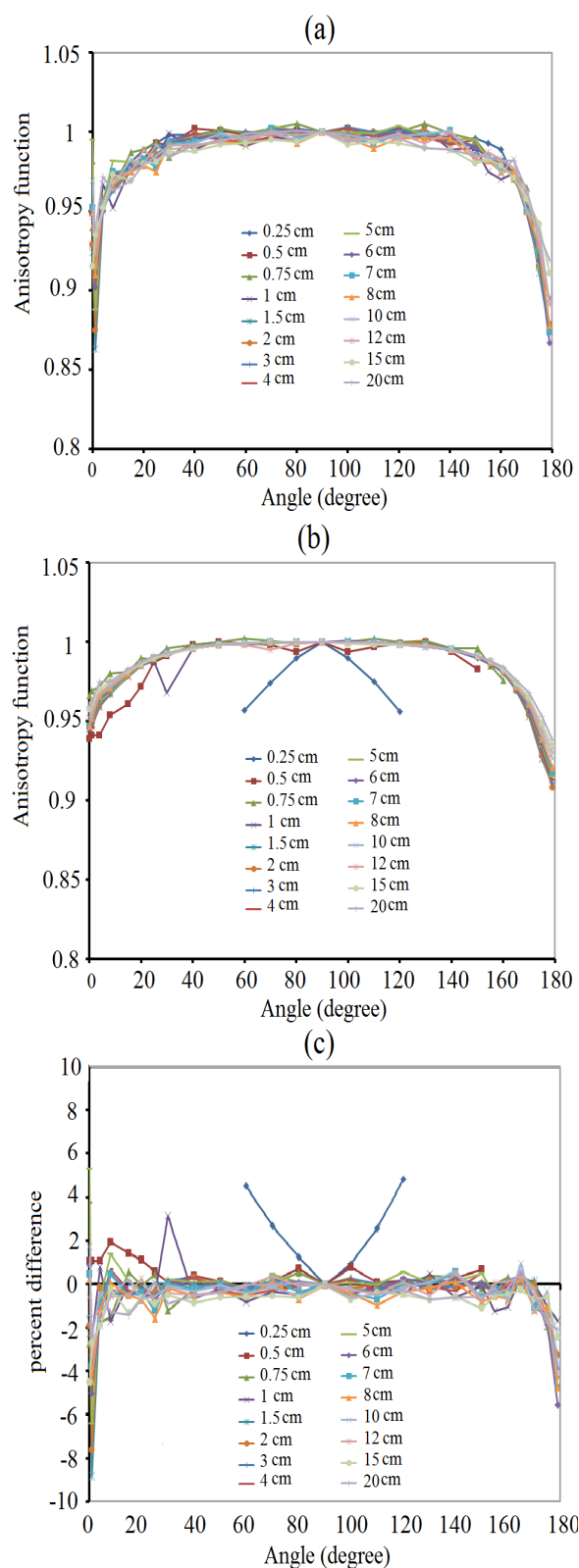


**Figure 2:** Anisotropy function for the Co0.A86  $^{60}\text{Co}$  source. (a): In the present study; (b): By Granero, et al.; (c): Percentage difference (%) between these two studies.

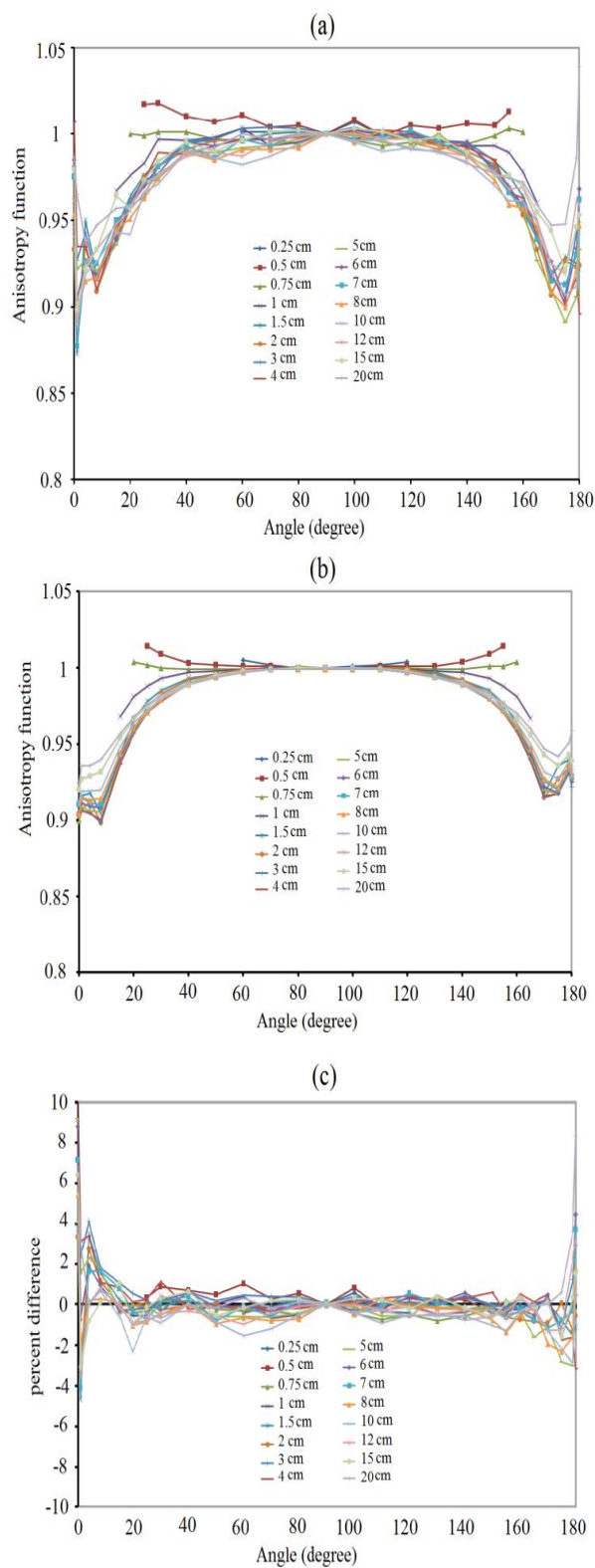


**Figure 3:** Anisotropy function for the 67-65200  $^{137}\text{Cs}$  source. (a): In the present study; (b): By Meigooni, et al.; (c): Percentage difference (%) between these two studies.

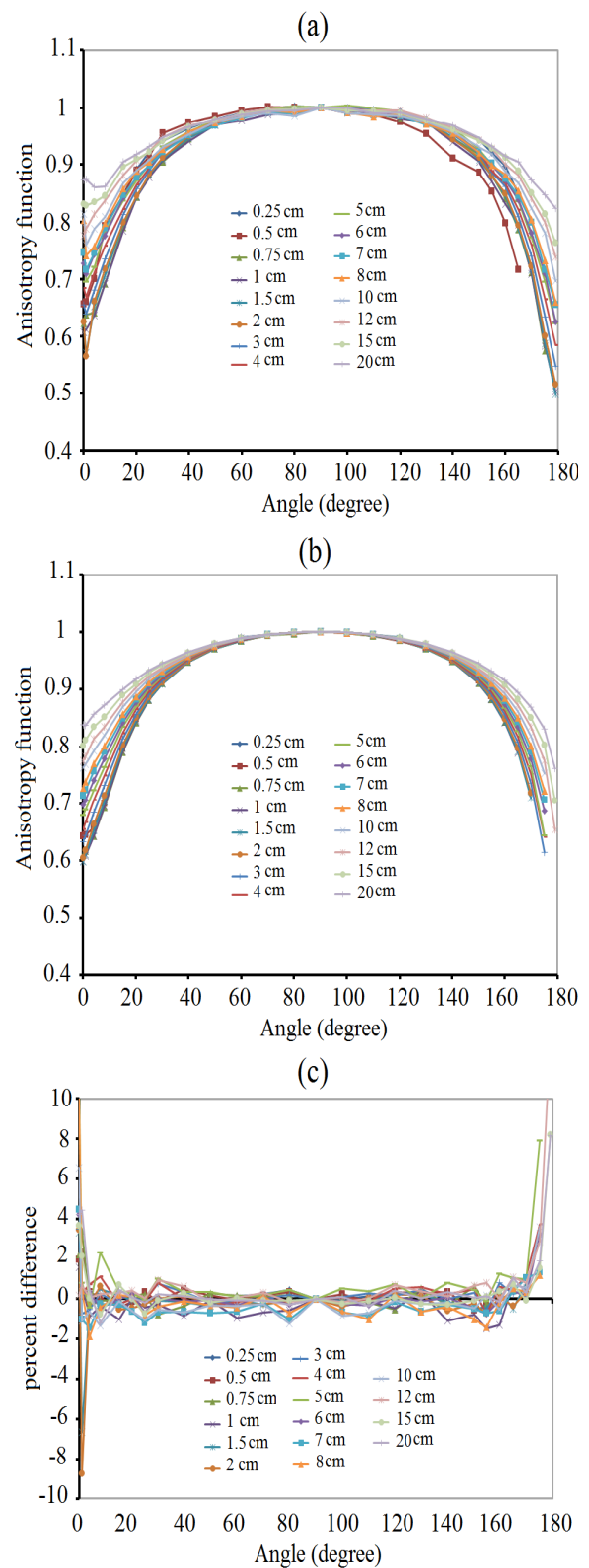


**Figure 4:** Anisotropy function for the BEBIG  $^{192}\text{Ir}$  source. (a): In the present study; (b): By Granero, et al.; (c): Percentage difference (%) between these two studies.

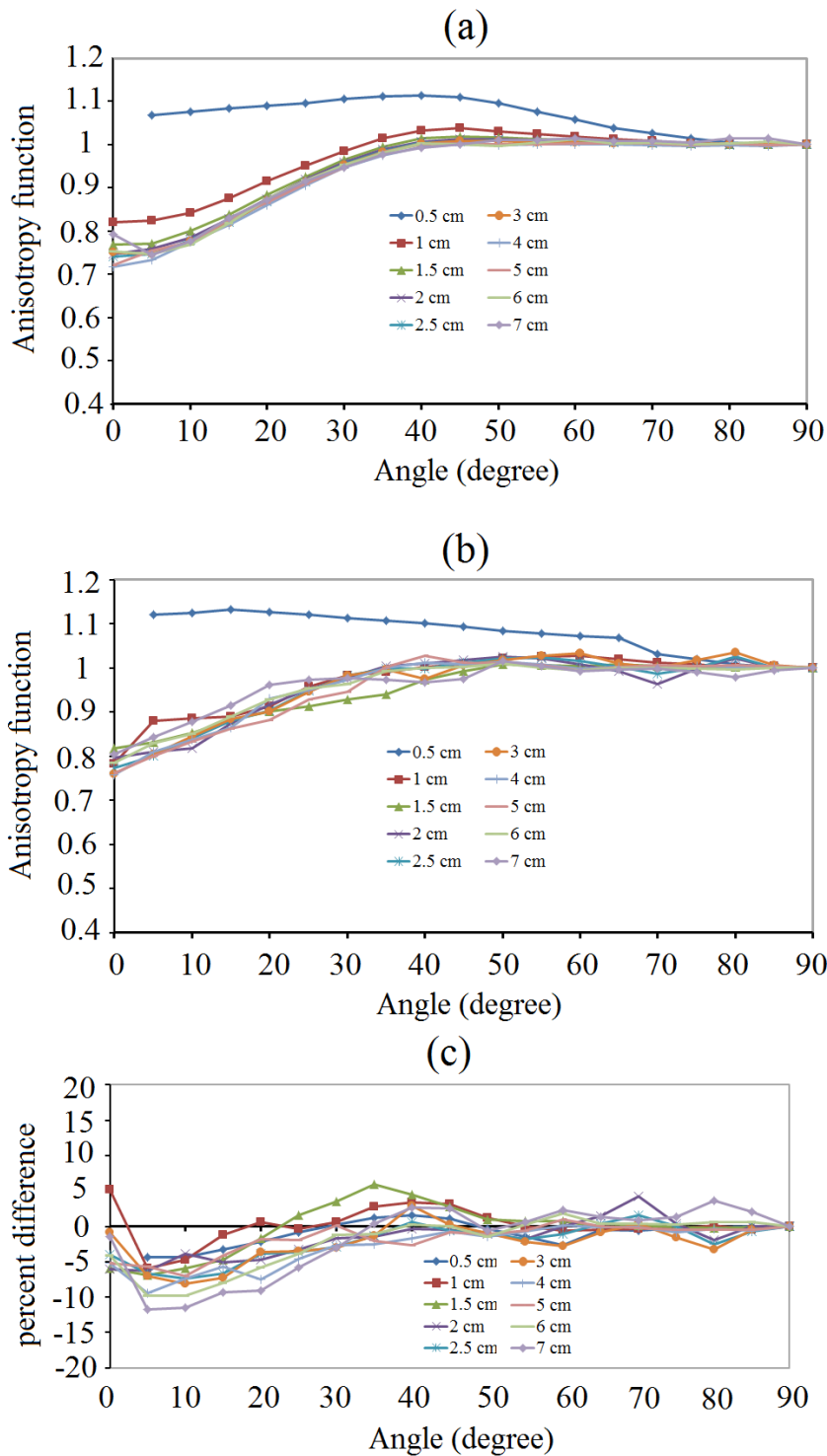


**Figure 5:** Anisotropy function for the OptiSeed <sup>103</sup>Pd source. (a): In the present study; (b): By Bernard and Vynckier; (c): Percentage difference (%) between these two studies.

differences between the anisotropy function values of the two studies are shown in Figure 4 (parts (c)). The maximum and mean absolute

percentage differences between the datasets from these two studies are 13.04% and 0.75%, respectively.

In Figure 5, anisotropy function values at different distances for the  $^{103}\text{Pd}$  source in this study and by Bernard and Vynckier are presented in parts (a) and (b), respectively. The percentage difference between the anisotropy function values of the two studies are shown in Figure 5 (parts (c)). The maximum and mean absolute percentage differences between the datasets from these two studies are 11.72% and 2.40%, respectively.

## Discussion

In the present study, TG-43 dosimetric parameters for Co0.A86  $^{60}\text{Co}$ , 67-65200  $^{137}\text{Cs}$ , BEBIG  $^{192}\text{Ir}$  and OptiSeed  $^{103}\text{Pd}$  brachytherapy sources were calculated and compared with the corresponding previously published data. The dosimetric parameters included air kerma strength, dose rate constant, radial dose function and the anisotropy function. The dose rate constant parameter values for the sources, as listed in Table 3, show good agreement with those corresponding values reported by Granero, et al., Meigooni, et al., Granero, et al., and Bernard and Vynckier. In Table 4, radial dose function values for the  $^{60}\text{Co}$ ,  $^{137}\text{Cs}$ ,  $^{192}\text{Ir}$  and  $^{103}\text{Pd}$  sources in this study are compared with other studies. One of the reasons for the high percentage difference for  $^{103}\text{Pd}$  source is its low-energy that causes fast fall-off of dose with distance around the source. As a result, dose decreases rapidly with distance from the source, and to calculate the percentage difference at far distances from the source, the denominator becomes small, then the percent difference becomes larger. In other words, lower dose in far distances from the source increases the percentage difference in these areas. In addition, there may be minor differences in simulation programs in various studies such as differences in cross-section library, size of the phantom, the energy spectrum and voxel size. For low energy sources, these differences result in large differences among the results of various studies. Similar levels of differences have been reported in other studies

for low energy sources.

According to Figures 2, 3, 4 and 5 show anisotropy function values for the four sources, in most of the data points the percentage differences between the two studies are less than 1%. These low levels of differences indicate good agreement between the anisotropy function data obtained in the present study and those reported by Granero, et al., Meigooni, et al., and Granero, et al. For the  $^{103}\text{Pd}$  source the percentage differences are higher, but there are other studies in which the same difference values were observed for  $^{103}\text{Pd}$  radionuclide as a brachytherapy source [13]. The comparisons also show a relatively good agreement between the anisotropy function from this study and those by Bernard and Vynckier for the OptiSeed  $^{103}\text{Pd}$  source.

The results of the anisotropy function in this study reveal a good agreement with other studies in most of the polar angles. However, higher percentage differences are observed in the low and high angles. Since the particles pass via larger distances inside the source and capsule at these angles than other angles, they are absorbed in a higher extent at low and high angles. Therefore, at these angles, few particles reach the scoring voxels and this results in higher statistical uncertainty in the simulations at these angles. To reduce the statistical uncertainty, simulation program should be run for more particle histories. To achieve this aim, there is a need for access to computers with higher data processing capabilities.

## Conclusion

The results for dosimetry parameters of dose rate constant, radial dose function and anisotropy function for the  $^{60}\text{Co}$ ,  $^{137}\text{Cs}$ ,  $^{192}\text{Ir}$  and  $^{103}\text{Pd}$  sources in this study demonstrated good agreement with other studies. Based on the good agreement between the results of this study and other studies, the TG-43 results for Co0.A86  $^{60}\text{Co}$ , 67-65200  $^{137}\text{Cs}$ , BEBIG  $^{192}\text{Ir}$  and OptiSeed  $^{103}\text{Pd}$  sources are validated and can be used as input data in treatment planning

systems (TPSSs) and to validate TPS calculations.

## Acknowledgment

The authors are grateful to Mashhad University of Medical Sciences for financial support of this work.

## Conflict of Interest

There is not any relationship that might lead to a conflict of interest.

## References

1. Suntharalingam N, Podgorsak EB, Tolli H. Brachytherapy: physical and clinical aspects. Podgorsak EB. Radiation Oncology Physics: a handbook for teachers and students. Vienna: International Atomic Energy Agency; 2005. p. 451-484.
2. Enger SA, Lundqvist H, D'Amours M, Beaulieu L. Exploring  $^{57}\text{Co}$  as a new isotope for brachytherapy applications. *Med Phys*. 2012;**39**:2342-5. doi.org/10.1118/1.3700171. PubMed PMID: 22559604.
3. Oliveira SM, Teixeira NJ, Fernandes L, Teles P, Vaz P. Dosimetric effect of tissue heterogeneity for  $^{125}\text{I}$  prostate implants. *Rep Pract Oncol Radiother*. 2014;**19**:392-8. doi.org/10.1016/j.rpor.2014.03.004. PubMed PMID: 25337412. PubMed PMCID: 4201780.
4. Williamson JF, Li Z. Monte Carlo aided dosimetry of the microselectron pulsed and high dose-rate  $^{192}\text{Ir}$  sources. *Med Phys*. 1995;**22**:809-19. doi.org/10.1118/1.597483. PubMed PMID: 7565372.
5. Rivard MJ, Butler WM, DeWerd LA, Huq MS, Ibbott GS, Meigooni AS, et al. Supplement to the 2004 update of the AAPM Task Group No. 43 Report. *Med Phys*. 2007;**34**:2187-205. doi.org/10.1118/1.2736790. PubMed PMID: 17654921.
6. Granero D, Perez-Calatayud J, Ballester F. Monte Carlo calculation of the TG-43 dosimetric parameters of a new BEBIG Ir-192 HDR source. *Radiother Oncol*. 2005;**76**:79-85. doi.org/10.1016/j.radonc.2005.06.016. PubMed PMID: 16019091.
7. Mowlavi A, Binesh A, Moslehitarbar H. Dose distribution and dosimetry parameters calculation of MED3633 palladium-103 source in water phantom using MCNP. *Iran J Radiat Res*. 2006;**4**:15-9.
8. Pérez-Calatayud J, Granero D, Ballester F, Puchades V, Casal E. Monte Carlo dosimetric characterization of the Cs-137 selectron/LDR source: Evaluation of applicator attenuation and superposition approximation effects. *Medical physics*. 2004;**31**:493-9. doi.org/10.1118/1.1644640. PubMed PMID: 15070245.
9. Granero D, Perez-Calatayud J, Ballester F. Technical note: Dosimetric study of a new  $^{60}\text{Co}$  source used in brachytherapy. *Med Phys*. 2007;**34**(9):3485-8.
10. Meigooni AS, Wright C, Koona RA, Awan SB, Granero D, Perez-Calatayud J, et al. TG-43 U1 based dosimetric characterization of model 67-6520 Cs-137 brachytherapy source. *Med Phys*. 2009;**36**:4711-9. doi.org/10.1118/1.3224462. PubMed PMID: 19928102.
11. Bernard S, Vynckier S. Dosimetric study of a new polymer encapsulated palladium-103 seed. *Phys Med Biol*. 2005;**50**:1493-504. doi.org/10.1088/0031-9155/50/7/012. PubMed PMID: 15798339.
12. Perez-Calatayud J, Ballester F, Das RK, Dewerd LA, Ibbott GS, Meigooni AS, et al. Dose calculation for photon-emitting brachytherapy sources with average energy higher than 50 keV: report of the AAPM and ESTRO. *Med Phys*. 2012;**39**:2904-29. doi.org/10.1118/1.3703892. PubMed PMID: 22559663.
13. Li Z, Palta JR, Fan JJ. Monte Carlo calculations and experimental measurements of dosimetry parameters of a new  $^{103}\text{Pd}$  source. *Med Phys*. 2000;**27**:1108-12. doi.org/10.1118/1.598975. PubMed PMID: 10841416.